Chapter 5
Electro-Magnetic Nano-Positioning

Zhuo Zhang, Yueqing Yu, Xinyu Liu, and Xuping Zhang

Abstract Electro-magnetic actuation technology has the potential of providing millimeters of actuation range with nanometers of positioning resolution, and recently has received increasing attention in the field of nano-positioning. Compared with other types of nano-positioning systems that are driven by electrostatic, thermal, and piezoelectric actuators, the electro-magnetic nano-positioning systems are able to achieve large power density with low input voltages, are capable of operating in large distances with virtues of linear response, and are featured with multi-axis actuation capability and with high bandwidth. Therefore, a variety of electro-magnetic nano-positioning systems have been developed for various nano-scale applications. Although electro-magnetic nano-position systems are equivalent in positioning objects in nano-scale, they could be different in size, configuration, degrees of freedom, fabrication process, and control scheme for being suited to certain application requirements. However, electro-magnetic nano-positioning systems generally consist of three essential parts: an electro-magnetic actuator, a guiding mechanism, and a positioning stage. Instead of covering all the aspects on either the various types of systems or the applications, this chapter presents the common and general principles of electro-magnetic nano-positioning systems: actuation, guiding mechanisms, kinematics, dynamics, control, and fabrication. The typical systems and applications in the literature are employed as examples to illustrate the common principles. The aim of the chapter is to provide readers with insight and guidance on the development of electro-magnetic nano-positioners.

5.1 Overview

Compared with other actuation types available such as electrostatic, thermal, and piezoelectric, etc., electro-magnetic actuations require low operation voltages, moderate power density, large operating distances, linear response, multi-axis capability, and high bandwidth [1]. These advantages make electro-magnetic nano-

Z. Zhang • Y. Yu • X. Liu • X. Zhang (✉)

Department of Engineering and Aarhus School of Engineering, Aarhus University, Inge Lehmanns Gade 10, 8000 Aarhus C, Denmark
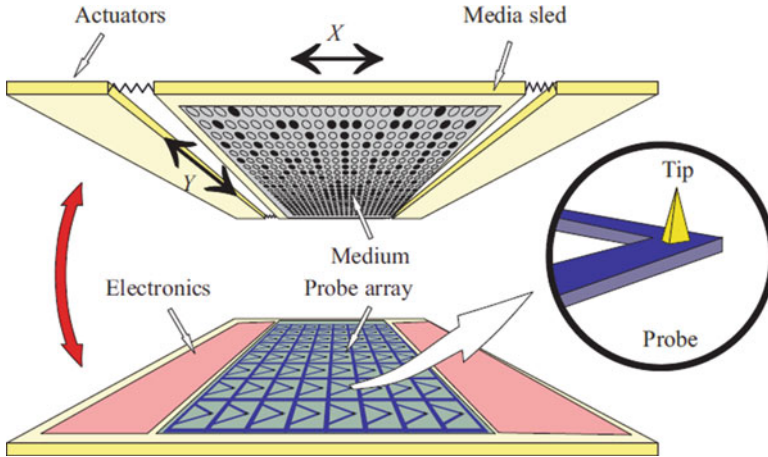e-mail: xuzh@ase.au.dk

Fig. 5.1 Schematic diagram of the principle of probe-based data storage [6]

positioning systems increasingly attractive over the recent decades. There are emerging applications and techniques that could benefit from nano-positioning technology, such as the scanning probe microscopy (SPM) [2], probe-based data storage (PDS) [3, 4], and nano-scale electro-machining (nano-EM) [5], etc. This chapter is devoted to an overall introduction of the fundamental principles and guidance on the analysis, design, control, and fabrication of the electro-magnetic nano-positioning technology, i.e., nano-positioning apparatus driven by electro-magnetic actuators.

One application is the PDS that has been proposed in the late 1990s. This technology has emerged from SPM, where a surface is scanned and manipulated at the atomic level to form topographic images [6, 7]. This data storage system is MEMS-based, which is comprised mainly of two separate layers, as shown in Fig. 5.1 [6]. The upper layer depicted in Fig. 5.1 is the medium layer, on which data will be recorded or removed, whereas the other layer carries an array of probes (or heads, usually several thousands) that is used to read/write/erase data via scanning and contact with the medium. There are two main scanning configurations for PDS, i.e., (a) probe-scanning, where the probe moving relative to a fixed medium layer, and (b) medium-scanning, where the medium layer is movable while the probe layer remains stationary. Usually the tip size of the probes is atomic-scale, resulting in the data bits are approximately 15 nm in diameter and the tracking pitch of 30 nm. A pit that was written into the surface and the original surface represent logical "1" or "0," respectively. In order to achieve data storage with high performance such as ultrahigh storage density, high speed, and suited to portable applications, the nano-positioning system must meet a stringent set of requirements. For example, to ensure extremely high data throughputs, a sufficient scanning range, high bandwidth, as well as reliable nano-scale positioning accuracy are needed. In addition, the portable storage applications also require lower energy consumption and vibration resistant capabilities.

Fig. 5.2 Nano-scale electro-machining process [8]
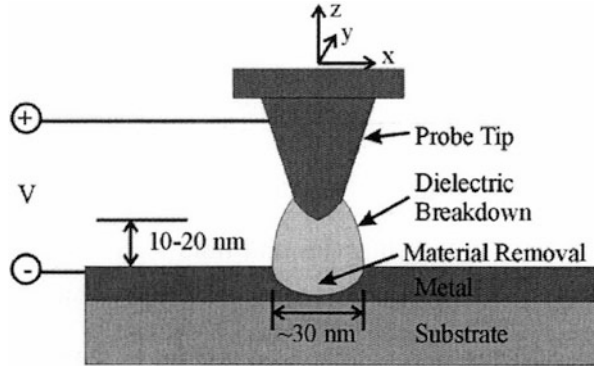
Another important emerging application benefited from the nano-positioning technology is probe-based nano-scale electro-machining (nano-EM). This technique modifies a surface at nano-scale through removing conductive material from the work surface. The process is illustrated in Fig. 5.2 [8]. The gap between the probe and the work surface is filled with dielectric. When sufficient high electric potential is applied, the dielectric will breakdown resulting in removal of local material from the work surface. In nano-EM, the positioner must control the probe-tip location and orientation relative to the surface in all six degrees of freedom (DOFs), i.e., three translation DOFs: x, y, and z and three rotational DOFs: θ_x, θ_y, and θ_z. In addition to having the nanometer-level or better resolution, the nano-EM process also requires good repeatability and short execution time to make the technology practical and competitive.

Electro-magnetic nano-positioning technology enables us to move large or small objects in nanometer-level or better precision, however, the actual positioner is not necessarily be on nano-scale. The dimensions range from macro- [9] to meso- [8] and even micro-scales [10, 11] based on various application purposes. Macro-scale nano-positioners can easily operate over large distances (100s microns to centimeters) and exert large forces (N-kN) with nanometer precisions. One typical macro device is the magnetic levitation system [12–14], which achieve nanometer-level precision thanks to its non-contact nature. It eliminates mechanical friction, stiction, backlash, and hysteresis that are detrimental to precise control. In addition, the macro-sized system is well capable in integrating sensing and feedback systems in order to stabilize their motion and ensure nano-scale precision. However, the sensing and feedback control add complexity to the design and assembling of the system. The large mass leads to low natural frequencies and bandwidth. This limits applications where high throughput is needed. On the other hand, macro-scale nano-positioners often consume more energy, and exhibit more thermal growth that may cause thermal instability and errors. A macro six-axis nano-positioning device with magnetic levitation technology is shown in Fig. 5.3 [9].

Although macro-sized devices are capable of positioning objects in nano-scale, they are not amenable to massively parallel operation resulting in low throughput
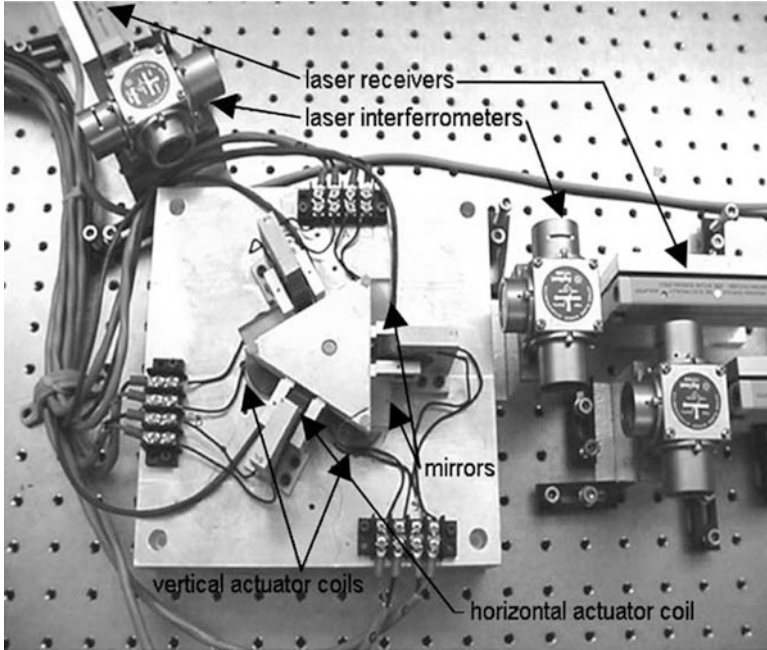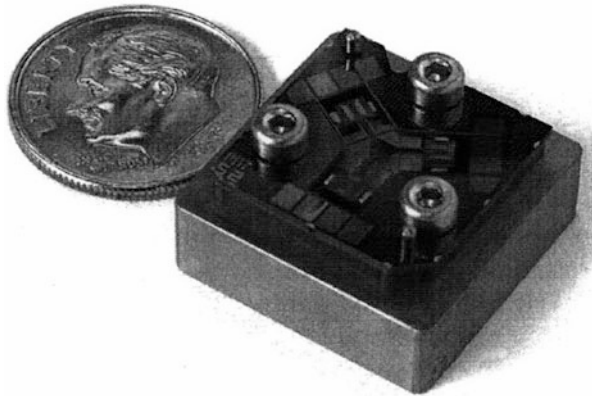
Fig. 5.3 Photograph of the six-axis maglev nano-positioning device [9]

Fig. 5.4 Image of an
x-axis meso-scale
electro-magnetically driven
nano-positioner developed by
MIT. The dime is included for
size reference [8]

rates. The great mass and volume limit the use for portable applications. Recent
years, researchers from Massachusetts Institute of Technology (MIT) developed a
six-axis meso-scale nano-positioner driven by electro-magnetic actuators, as shown
in Fig. 5.4 [8]. This device is only centimeters in size with the central stage driven
by three sets of integrated electro-magnetic actuators. Due to the reduced size, it is
possible to run several nano-positioners in parallel to achieve high throughput rates.
Moreover, the reduction in mass makes it much easier to attain higher mechanical
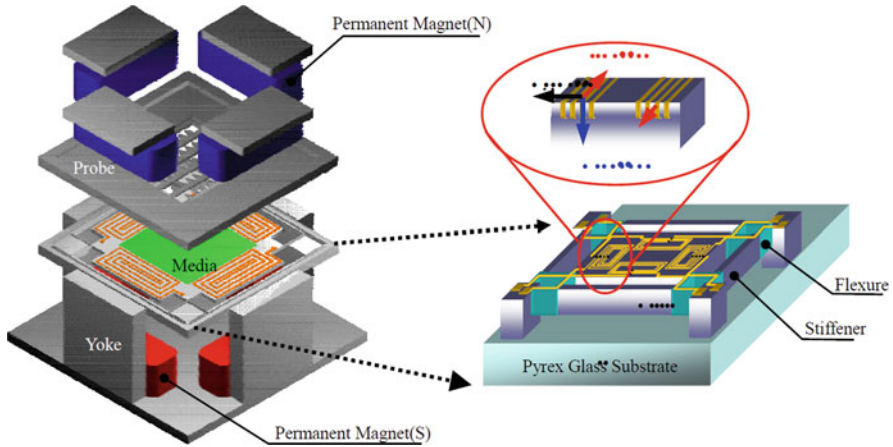
Fig. 5.5 Structure of probe-based data storage (PDS) with electro-magnetic micro *x*–*y* stage and its working principle [10]

bandwidth of the system. Also, meso-scale nano-positioners exhibit less thermal growth, cost less energy, and cause smaller thermally-induced errors accordingly than macro counterparts. However, several challenges must be overcome as the size is significantly scaled down. For example, design and integration of meso-scale multi-axis electro-magnetic actuators are totally different from macro devices. The assembling of position and orientation sensors is a big challenge.

With the maturation of MEMS (Micro-Electro-Mechanical System) technology, electro-magnetic nano-positioner can be scaled down to millimeter scale. Figure 5.5 shows a micro-scale nano-positioner for PDS application. The size of the media platform is 5×5 mm^2. The micro-scale positioner is compatible and portable. However, due to their small size it is difficult, if not impossible, to integrate sensors, and it is challenging to design a micro stage with up to six DOFs.

Despite their differences in size, the macro, meso, and micro electro-magnetic nano-positioner share a common operation principle and structure. The positioning system mainly consists of a stage, electro-magnetic actuation parts, and a guiding part that links the actuation parts to the stage. The purpose of this chapter is to introduce common principles on how electro-magnetic actuations could generate stage motions with nanometer precisions. Based on the principles and different applications, we will also point out key considerations on design, control, and fabrication. This chapter will not be confined to certain types of electro-magnetic nano-positioning systems, instead, it will provide potential readers with the basic principles, methodologies, and fundamental considerations on this topic.

5.2   Principle of Electro-Magnetic Actuation

5.2.1   Actuation Force Generation

In general, the electro-magnetic actuation parts consist mainly of one or several pairs of permanent magnets and coils. Upon the application of a current in the coil, the associated magnetic field of the coil is generated. In presence of the magnetic field generated by permanent magnets, the output actuation forces are generated thanks to the attraction and/or repel forces between coils and permanent magnets.

5.2.1.1   Solenoid

Solenoid is often used along with a permanent magnet to generate actuation forces based on magnetic attraction and/or repulsion effect. Solenoid behaves like a long bar magnet of which the north and south pole of the magnetic field is governed by right-hand rule, as shown in Fig. 5.6. There are a variety of applications benefited from solenoid such as electro-magnetic lifting machine, the electric bell, the electro-magnetic relay, and telephone earpiece, etc.

Based on Ampere's Circuital Law, the magnetic field of solenoid is expressed as

$$B = \mu_0 IN/L \tag{5.1}$$

where μ_0 is called the permeability of free space, I the input current, N the number of turns, i.e., number of loops the solenoid has, and L the length of solenoid. The strength of the magnetic field can be increased by the four approaches: (1) increasing the current; (2) increasing the number of turns; (3) placing a soft iron rod/core inside the solenoid; and (4) pushing the turns of the wire closer to make north and south poles closer. In practice, for positioning applications, the magnetic strength (actuation force) is governed by the control of input currents. In addition to the magnitude of the passing current, the direction of the current determines the direction of north and south poles and the direction of actuation accordingly.

The main shortcoming of the solenoid-based actuation is the difficulty to fabricate and assemble meso- and even micro-scale solenoids. They are used

Fig. 5.6 Solenoid and right-hand rule
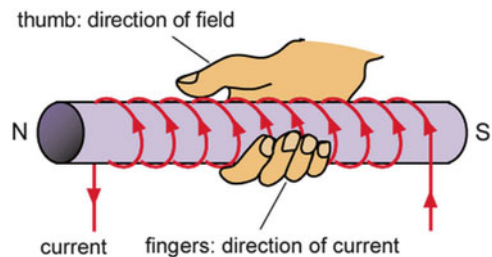
alone in macro-scale magnetic levitation systems for nano-positioning. Moreover, solenoid-based electro-magnetic actuators can only achieve one-axis motion, which limits their uses when multi-axis actuation is desired. These drawbacks are induced mainly by the spatial structure of the solenoid. To overcome this, planar-coil electro-magnetic actuation schemes have been employed in nano-positioning systems. To help reader better understand the actuation principles, the physical principle of Lorentz force and Ampere's force is briefly introduced as below.

5.2.1.2 Lorentz Force and Ampere's Force

In presence of only a magnetic flux $\mathbf{B}$, and electric charge q moving with a velocity $\mathbf{v}$ experiences a magnetic force $\mathbf{F_m}$. The magnetic force is called Lorentz force and is expressed as

$$\mathbf{F_m} = q\mathbf{v} \times \mathbf{B} \tag{5.2}$$

The magnetic force $\mathbf{F_m}$ affects only the direction of motion of q, not the kinetic energy. Because the direction of magnetic force is perpendicular to the velocity of q and does no work. Electric current is motion of charge. To make Lorentz force practical, Ampere's force has been employed which refers to the force exerts on the current-carrying wire in a magnetic field. The Ampere's force, total force acting on the wire, is

$$\mathbf{F} = \int_{\text{wire}} I d\mathbf{L} \times \mathbf{B} \tag{5.3}$$

where I represents electric current and $d\mathbf{L}$ refers to differential elements of length of the wire. Figure 5.5 shows a planar-coil-based electro-magnetic micro x–y stage, in which the Lorentz force/Ampere's forces used to actuate the stage. Usually, the magnetic field is created by permanent magnets, and thus the magnitude and direction of the magnetic force are determined by electric current.

5.2.2 Configurations

5.2.2.1 Magnet-Moving Versus Coil-Moving

In generating actuating force, two configurations of electro-magnetic actuator have been adopted: magnet-moving and coil-moving. Moving magnet actuations operates with the coil fixed and the magnets moves for actuation, whereas the moving coil systems works by fixing the magnets to the base and the coils are moved for actuation. A typical moving magnet system is shown in Fig. 5.7 [15], where the coils are fixed and the magnets are mounted on a flexure guiding mechanism. Fixing
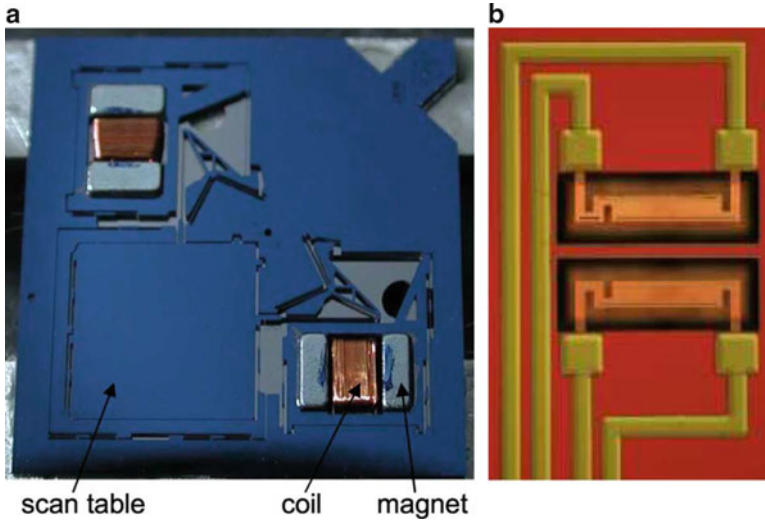
Fig. 5.7 (**a**) Photograph of a prototype nano-positioner for probe-based data storage and (**b**) the thermal position sensors [15]

the coils is ideal for thermal dissipation and therefore higher operating currents are allowed and larger actuation forces are achieved. However, the magnets must be bonded onto the flexure mechanisms, which is a challenging work especially for meso- and micro-scale devices. Another drawback inherent in magnet-moving design is that the magnets are in general a big mass which results in lower bandwidth of the actuators.

In contrast, for coil-moving configurations, as shown in Fig. 5.5, it is easier to achieve high bandwidth since the mass of coils can be decreased by virtue of micro-fabrications. However, for applications that require sufficient precision, the heat dissipation from the moving coil through the flexure mechanism will cause thermal-induced errors. To reduce the thermal-based errors, the operation current must be kept in lower magnitude for coil-moving configurations. As a result, such configurations can only provide less actuation force compared with magnet-moving configurations.

5.2.2.2 Single-Axis and Multi-Axis

Most of applications for nano-positioning require at least two degree-of-freedom, such as planar scanning. Some applications require up to six degree-of-freedom (DOF), such as nano-EM. For this purpose, electro-magnetic actuators must have one-axis or multi-axis capabilities, and need to be appropriately arranged. In general, for the purpose of achieving the positioning stage with multiple DOFs, either the choices of more actuators with less axes or less actuators with more
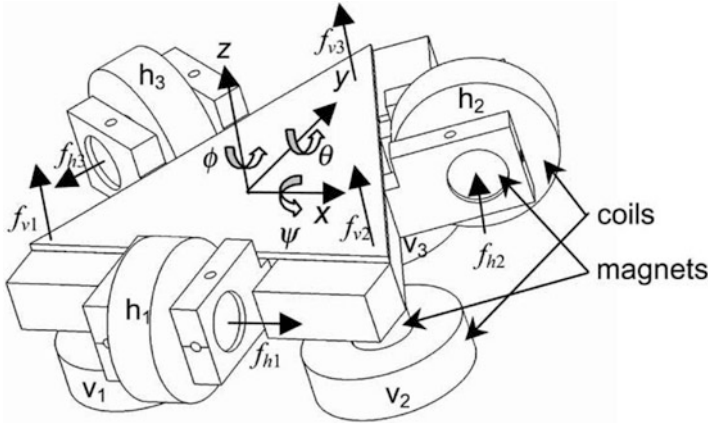
Fig. 5.8 A six DOFs nano-positioning device driven by six single-axis actuators [9]

axes is feasible. Fewer axes for each actuators will facilitate design of actuators with a compromise that the design of guiding mechanism and actuator arrangement become complex. On the contrary, more axes for each actuators may add complexity of actuator design but make design of guiding mechanism and actuator arrangement with ease. However, to the best knowledge of the authors, no efforts have been devoted to the development of electro-magnetic actuators having more than two-axis.

The six-axis magnetic levitation nano-positioning device shown in Fig. 5.3 has six independent single-axis electro-magnetic actuators, of which the detailed arrangement is seen in Fig. 5.8 [9]. In order to achieve six-DOF positioning of the stage, three actuators are combined to generate in-plane motion, and the rest of the three actuators are responsible in producing out-of-plane motions. Another six-DOF stage developed by MIT is shown in Fig. 5.4, where only three actuators with double-axis are incorporated. Each actuator provides two mutually perpendicular axial motions, i.e., in-plane and out-of-plane, as shown in Fig. 5.9. The three ways actuations simplified the guiding mechanisms that connect the actuators and the center stage. As a tradeoff, it adds complexity in design, fabrication, and assembling of each actuators.

As illustrated in Fig. 5.10 [16], in achieving both in-plane and out-of-plane motions, two separated coil layers are stacked. The stacked configuration is benefited from the planar coil-moving scheme. The actuation force is generated thanks to Lorentz force/Ampere's force via interaction of the coil current with the permanent magnet field.

Fig. 5.9 A six DOFs
nano-positioning device
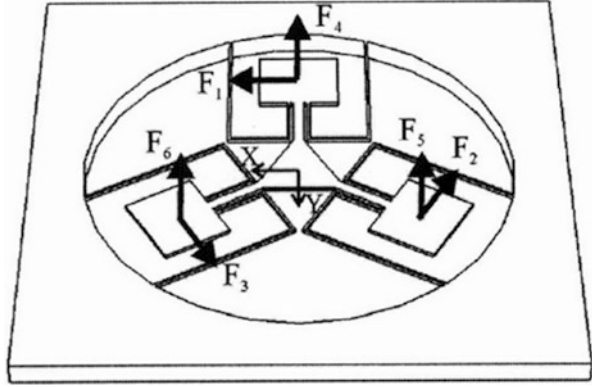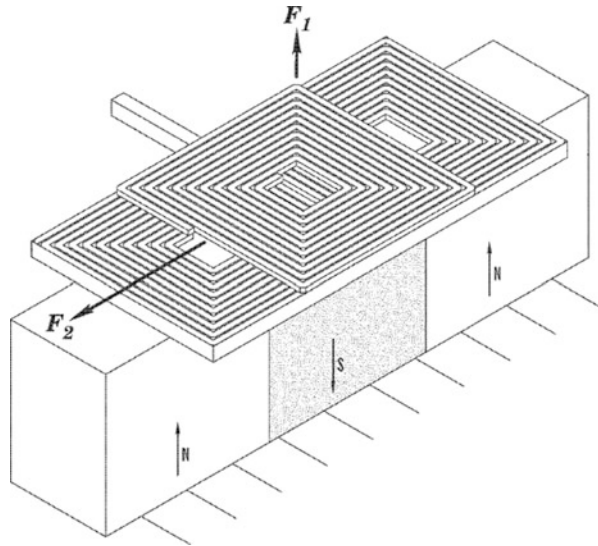driven by three double-axis
actuators [8]

Fig. 5.10 Schematic diagram
of a double-axis
electro-magnetic actuator
[16]

5.3 Compliant Guiding Mechanisms

Guiding mechanisms enable motion guidance of individual actuators to form the
stage motion. There are two main categories of the guiding mechanisms: (1)
the rigid mechanisms which use prismatic and rotational kinematic joints for
bearing and guidance, as shown in Fig. 5.8; (2) the compliant mechanisms (i.e.,
flexure mechanisms) which transfer or transform motion, force, or energy via
elastic deformations, as shown in Figs. 5.5 and 5.9. Compared with rigid guiding
mechanisms, the compliant counterparts are more favorable particular in meso- and
micro-scale applications. Since fabrication and assembling of rigid mechanisms
are challenging and rigid mechanisms will incur backlash, inaccuracy in motion,
frictions, and wear because of the rigid prismatic and rotational joints. In contrast,

the compliant mechanisms have advantages in two categories: cost reduction (part-count reduction, reduced assembly time, and simplified manufacturing processes) and increased performance (increased precision, increased reliability, reduced wear, reduced weight, and reduced maintenance) [17]. These virtues ideally fulfill the requirements as the size of electro-magnetic nano-positioner decreases. Moreover, this compliant structure enables stabilization without the feedback aids. There are also some challenges associated with compliant guiding mechanisms such as hysteresis, sensitivity to overloading, thermal sensitivity, and low range of motion, etc. In this section, we will provide readers with key methodologies and considerations in designing the compliant guiding mechanisms.

5.3.1 Design Considerations

Recent efforts in compliant guiding mechanisms are based on intuitions, for which the beams with constant sectional area are usually used. Upon operation and analysis, small and linear deformations are assumed. In designing the compliant guiding mechanisms for electro-magnetic nano-positioning systems, the finite-element analysis is used to obtain the force-deformation relationship, transmission ratio, thermal response, and stress, etc. In what follows, we list some key design considerations that can be used as a reference in achieving high nano-positioning performances for a variety of applications.

5.3.1.1 Distributed and Lumped Compliant Mechanisms

Distributed compliant mechanisms are those structures that they are flexible at every position, whereas the lumped compliant mechanisms are those consists of both rigid and flexible parts. For distributed compliant mechanisms the final position is determined by accumulation of deformations at every position. One typical geometry of distributed compliant mechanisms is the beam with uniform cross-sectional areas. As shown in Fig. 5.9, three sets of double-bent beams are used to support the stage and actuators and guide motions. In contrast, the final position of a lumped compliant mechanism is guided thanks to deformation of flexible hinges [18]. Different types of hinges provide unique properties to suit different requirements. Here we present three commonly used flexible hinge forms, i.e., the circular, the corner-filleted, and the elliptical hinges, as shown in Fig. 5.11 [19].

The circular hinge is superior to the others in achieving accurate rotational motions with high out-of-plane deflections. The center of deflection can be estimated to be at the center of the hinge. However, the high precision is only limited to a relatively small range. The corner-filleted hinge has relatively low bending stiffness. The performances of elliptical hinges are in between the circular and corner-filleted ones. For the same deflection, elliptical have lower maximum stress than corner-filleted ones resulting in a longer fatigue life. Besides the three
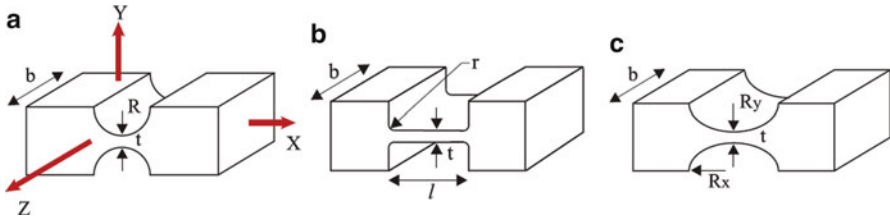
Fig. 5.11 Different types of hinges. (**a**) Circular, (**b**) corner-filleted, and (**c**) elliptical [19]
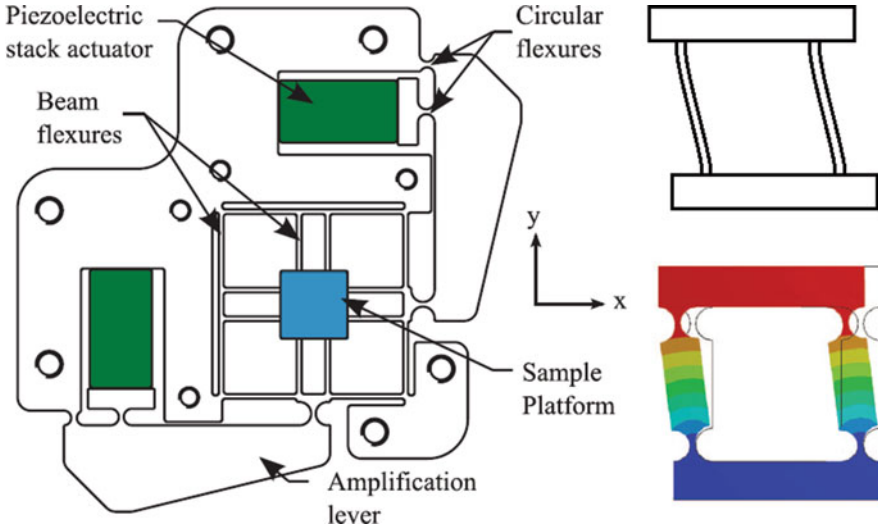

Fig. 5.12 Compliant parallel-guiding mechanisms in positioning application [19]

Table 5.1 A comparison of different flexure hinges [19]

Flexures	Stiffness		Motion accuracy	Max. stress
	In-plane	Out-of-plane		
Circular	High	High	High	High
Corner-filleted	Low	Low	Low	Low–med
Elliptical	Low–med	Low–med	Med–high	Low
Parabolic	Med–high	Med–high	Med–high	Med
Hyperbolic	High	High	High	Med–high

commonly used hinges, there are other flexure hinges available such as parabolic and hyperbolic. Details of the performances of those hinges are listed in Table 5.1 [19].

One typical compliant mechanism called compliant parallel-guiding mechanisms has been used in positioning applications, as shown in Fig. 5.12 [19], in which two opposing links remain parallel throughout the mechanisms motion. In this regard,

the parallel-guiding mechanisms produce alone the translation motion without a rotation motion exerting on the stage. To this end, the opposing links must be fabricated with the same length and form a parallelogram. This compliant four-bar mechanism can be either fully- or partially-compliant designed.

5.3.1.2 Stiffness and Resonant Frequency

The stiffness of the compliant guiding mechanisms determines the range of motion and resonant frequencies of the nano-positioner. For general cases, the compliant guiding mechanisms are used only confined to the linear elastic assumptions, where the positioning system can be treated as a linear mass-spring model. With this, the static displacement and resonant frequency of the system are given by [8]

$$F = k\delta \tag{5.4}$$

$$f = \frac{1}{2\pi}\sqrt{\frac{k}{m}} \tag{5.5}$$

The static displacement and resonant frequency can be obtained for a value of stiffness. The stiffness of simple structures, such as uniform cross-sectional beams, can be derived using either Euler–Bernoulli theory or Castigliano's second theorem. For complex structures, finite-element methods are often used to obtain the stiffness. As can be seen in Eq. (5.4), for a force-limited actuation, a stiffer flexure leads to small range of motion. Equation (5.5) shows that for a given moving mass, a stiffer structure increases resonance frequency. Because the flexure structure deforms and stores potential energy, the resonance frequency will limit the bandwidth. As a result, the compliant guiding mechanisms should be designed neither too flexible nor too stiff. Another important concern is that the stiffness is sensitive to the fabrication errors, which may cause errors in the motion range and bandwidth.

5.3.1.3 Transmission Ratio and Coupling

The transmission ratio is defined as the ratio of the stage to actuation displacement in a given direction [8]. This concept is important in nano-positioning systems since structure of large transmission ratio will amplify the errors of the actuation causing large positioning errors in stage. The compliant guiding mechanisms may be designed to enable motion/error de-amplification for nano and even sub-nano-positioning applications. However, this de-amplification treatment will result in a limited range of motion.

For most cases, flexure-based systems will give rise to coupling problems, which is caused by non-zero stiffness of the flexures perpendicular to the direction of actuation. This will definitely change the transmission ratios and lead to additional parasitic motions.

5.3.1.4 Thermal Issues

For nano-motions, the thermal effects cannot be ignored [19]. As mentioned previously, for coil-moving configurations, the heat generates via Joule heating in the coils and dissipates through radiation, convection, and conduction. Among these, heat conduction to compliant guiding mechanisms predominates. The increased temperature will lead to thermal expansion effects, resulting in significant drift and positioning error. Careful material selection and mechanical arrangement are effective ways to minimize thermal expansion effects. Using the materials with small coefficient of thermal expansion (CTE) ensures less expansion with increased temperatures. Moreover, materials of high thermal conductivity should be selected in case that quick thermal equilibrium will be achieved. Proper arrangement of the compliant guiding mechanisms is essential in eliminating the thermal effects, which is presented in the following section.

5.3.1.5 Configurations

The configurations of compliant guiding mechanisms are considered at two aspects: function and performance. First, the configurations must fulfill the requirement that several actuations produce stage motions with certain number of DOFs. This is achieved by determining how many actuators with certain number of axes are used and how they should be allocated. Second, the arrangement of the compliant guiding mechanisms must ensure the positioning performance.

As mentioned previously, the thermal effects of the coil-moving actuator result in thermal drift and significant errors. In addition to a proper selection of materials, a symmetry structure is often employed for passive thermal compensation purpose, as shown in Fig. 5.13. In this scheme, the thermal drift and positioning errors are minimized because of the symmetric configuration. As a result, greater current can be applied on the coils and therefore the actuators can produce larger force without a loss of positioning error of the stage.
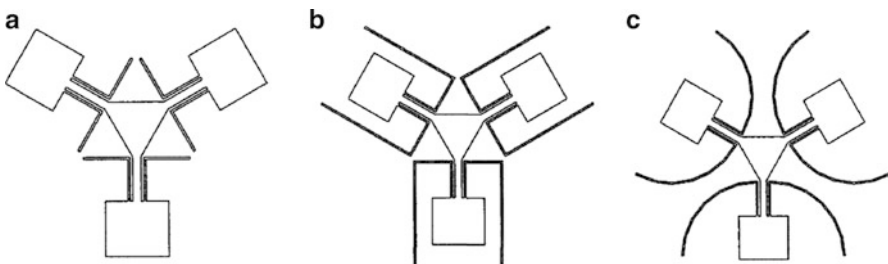

Fig. 5.13 Nano-positioner flexure concepts. (**a**) Single-bent beam, (**b**) double-bent beam, and (**c**) bow-flexure [8]

Figure 5.13 also illustrates three possible symmetric configurations, i.e., single-bent beam, double-bent beam, and bow-flexure [20, 21]. The geometric constraints limit the total length of the beams of the single-bent beam concept, which results in higher stiffness, higher resonant frequency, and lower transmission ratio over the other two concepts. The double-bent beam and bow-flexure share similar performances.

Compliant guiding mechanisms have the virtue of shock and vibration resistance because of their compliance. On the other hand, however, the compliant mechanisms must be designed stiffer to be robust against position errors caused by vibration and shock. To eliminate the shock and vibration effects on position errors and allow sufficient compliance for operations simultaneously, a mass balance concept is preferred. The nano-positioner in Fig. 5.7 is designed based on this concept, of which the one-dimensional illustration is shown in Fig. 5.14a [22]. In this configuration, if we apply an actuation force in the positive y-direction, as shown in Fig. 5.14b the compliant mechanisms will pull the table down in negative y-direction, making the dynamic effects of the actuator and the table balanced. When under shock conditions, as shown in Fig. 5.14c, an acceleration will be exerted on the whole structure. If $m_{actuator} \times x_1 = m_{table} \times x_2$, then the pivot, table, and actuator do not move relative to the frame. With this, the operation precisions of the nano-positioning system will not be affected by external shock and vibrations.
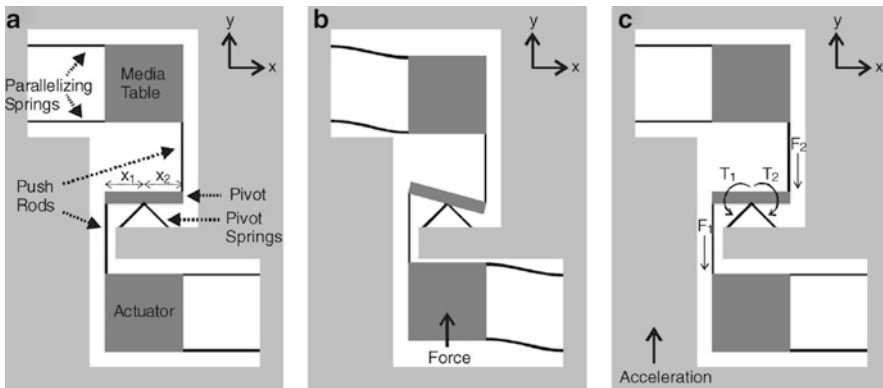

Fig. 5.14 (**a**) One-dimensional illustration of a mass balance positioner. (**b**) Rotation of pivot and displacement of the actuator and table due to the application of a force to the actuator. (**c**) Illustration of the forces and torques acting on the pivot resulting from the acceleration of the frame of the positioner [22]

5.3.2 Design Methods

The design of compliant guiding mechanisms is essential in achieving high performance for various positioning applications. However, current design of compliant guiding mechanisms stems from designer's intuitive and trial and errors. A lack of reliable and systematic design methods makes it not possible to design the compliant guiding mechanisms with optimal performance. Moreover, current designs are based on linear assumption of material properties. This is only adapted to small deformation applications and results in only a limited range of positioning motions. Thus in this section, we present two major design methods that is useful in the large deformation design and optimal design of the compliant guiding mechanisms.

5.3.2.1 Pseudo-Rigid-Body Model

Pseudo-rigid-body model is an efficient tool for analysis and design of compliant mechanisms with the assumption of large and nonlinear deflections [17]. Although there are other approaches available for large deflection problems such as elliptic integral and nonlinear finite-element methods, the formulations are cumbersome and solutions are time-consuming. The pseudo-rigid-body model, on the other hand, provides a rather simple method for large and nonlinear deflection modeling in that the rigid-link mechanism theory can be used to analyze and design the compliant mechanisms. The essential of the modeling concept is: the deflection of compliant mechanisms is modeled using rigid-body components, and the lumped springs are employed to simulate the equivalent force–deflection characteristics. Different compliant mechanisms require different pseudo-rigid-body models to accurately predict the deflection path and force–deflection relationships. In achieving this, the key issues of pseudo-rigid-body modeling are to decide where to place the pin joints and the value of the spring constants. In what follows, we present two common flexible segments that may be useful in design the compliant guiding mechanisms when large and nonlinear deflections are needed.

First we consider the small-length flexural pivots, as shown in Fig. 5.15 [17]. The beam consists of two segments: one is short and flexible, and the other is long and rigid. This beam can be treated as lumped compliant mechanism if the small segment is significantly shorter and more flexible than the large segment. In this case the pseudo-rigid-body model can be defined as shown in Fig. 5.16 [17], where the two rigid links joined at a pin joint. The pin joint is called characteristic pivot. The pivot can be put at any point along the flexible segment with no loss of accuracy because the length of the flexible segment is much small compared to that of the rigid link. For simplicity, however, the characteristic pivot is usually placed at the center of the short segment. Apparently, the accuracy of the model will be improved for the decreased length of flexible segment. The spring constant value can be found from elementary beam theory. The pseudo-rigid-model is more accurate if the bending is the dominant loading in the flexural pivot. If the transverse and axial
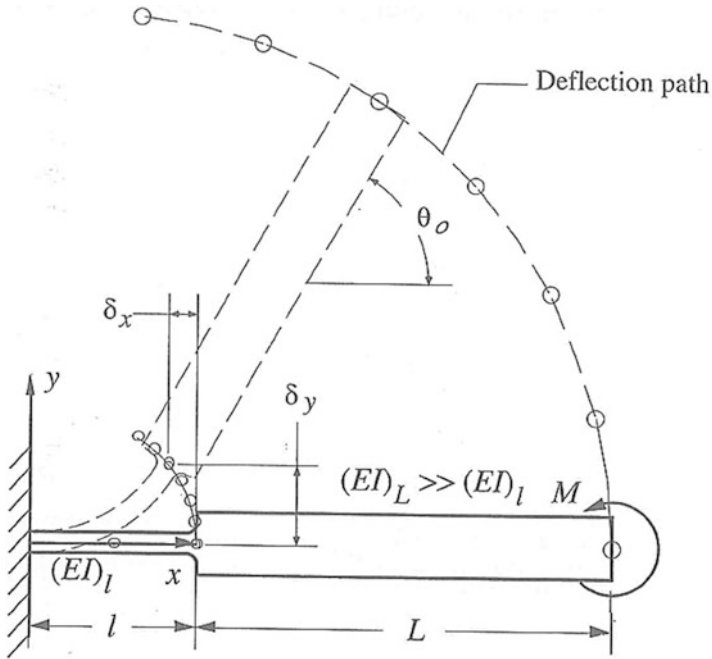
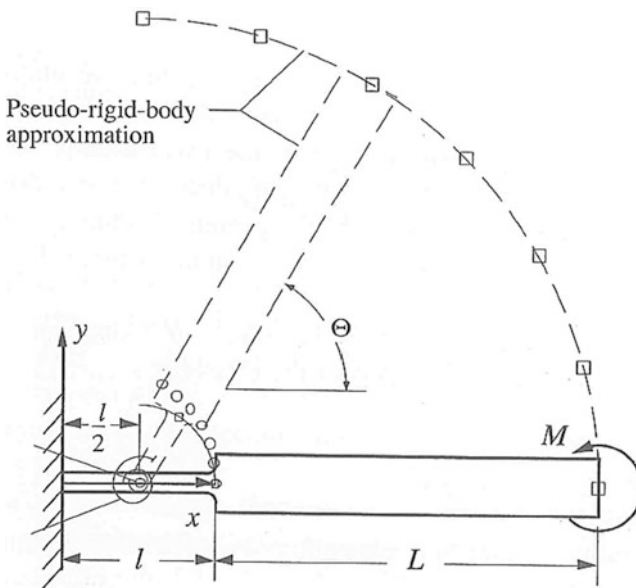**Fig. 5.15** Small-length flexural pivot [17]

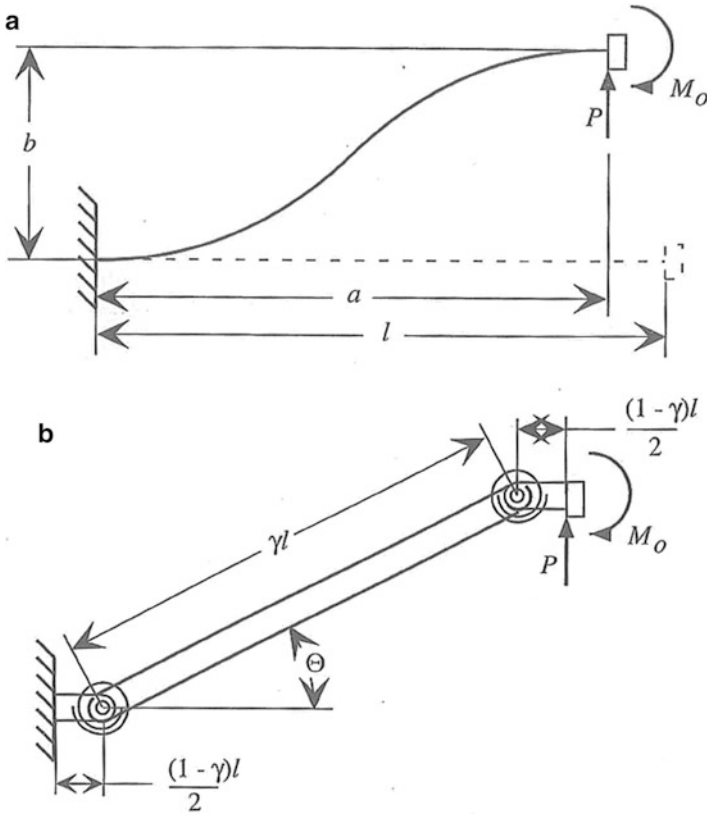**Fig. 5.16** Simple pseudo-rigid-body model of the small-length flexural pivot [17]

Fig. 5.17 (**a**) Fixed-guided flexible segment and (**b**) its pseudo-rigid-body model [17]

loads become significant, greater errors will be introduced using this simple pseudo-rigid-body model. Detailed descriptions of this model are presented in reference [17].

The electro-magnetic nano-positioning stages are often guided by the fixed-guided a flexible segment, as shown in Fig. 5.17a, of which one end of the beam is fixed while the other maintains at a constant angle. The associated pseudo-rigid-model is shown in Fig. 5.17b. Details of the pseudo-rigid-model can be found in [17]. It should be noted that for analysis and design of certain compliant mechanisms, the pseudo-rigid-body model is not unique. Actually, all the compliant mechanisms can be thought of as a sequence of infinite number of rigid bodies linked by springs. In modeling the compliant mechanisms, one has to make a compromise between the accuracy of the pseudo-rigid-body model and complexity of analysis and design. Fewer springs are preferred in pseudo-rigid-body model if it fulfills the accuracy requirements. As a result, the pseudo-rigid-body model conducts the analysis and design of the compliant mechanisms based on the methodologies used for rigid-body mechanisms. The modeling method is not only

suited to the kinematics but also the dynamics of compliant mechanisms. The main drawbacks of the pseudo-rigid-body model is that it only applies to compliant structure with regular geometry such as beams with constant cross-sectional area so that the elementary beam theory can be used to determine the stiffness constant.

5.3.2.2 Optimal Synthesis with Continuum Models

As mentioned, pseudo-rigid-body model and beam theory are suited only for structure that has regular geometry. However, for compliant mechanisms design, the structural geometry is not necessarily to be regular. Analysis, modeling, and design of compliant mechanisms with irregular geometry can be accomplished by using continuum model instead [23–25]. Based on continuum solid mechanics, structural optimization techniques can be used for compliant mechanisms design. By specifying the desired force–deflection behavior, materials, and design domain (i.e., the region the mechanism to be designed must fit), the structural optimization method generates the optimal solution automatically. The optimal design can be based on many design criteria such as maximum stiffness, minimum weight, suitable flexibility, and natural frequency, etc. For irregular geometries, the elastic deflection behavior is governed by partial differential equations, of which closed-form solutions are not possible. These equations are solved using numerical methods such as finite-element method, finite difference method, boundary element method, etc. The detailed introduction of this method can be found in [17].

5.4 Kinematics and Dynamics

Previous sections introduce the design issues of the two main components of the electro-magnetic nano-positioning systems, i.e., the electro-magnetic actuators and the guiding mechanisms. In the analysis and design of a whole electro-magnetic nano-positioning system, however, the primary issue is the kinematic analysis, for example, deciding how many actuators with single- or multi-axes are required in achieving stage motions with certain DOFs, and how the actuators should be arranged. In view of control, it is important to understand that how these actuators should be controlled in achieving desired motion. In addition to kinematics, some dynamics issues should also be taken into account.

5.4.1 Degrees of Freedom

The DOFs of the positioning system is essential in the study of kinematics and dynamics. In general, stage motion with several DOFs requires at least an equal number of properly arranged independent actuation inputs [26]. Unlike traditional
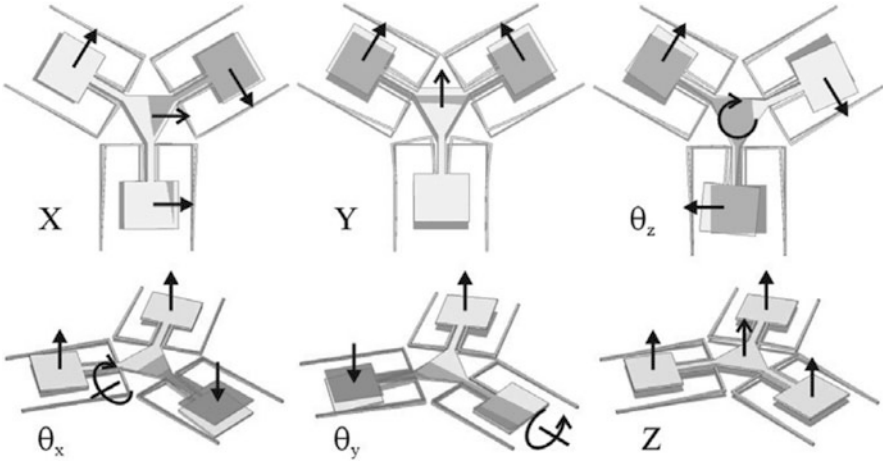
Fig. 5.18 Working principle of a six-axial positioning stage [27]

mechanisms that is capable of achieving rotations by directly using the rotation actuators. The rotation motion of the electro-magnetic nano-positioning stage is only accomplished based on the couple, because the electro-magnetic input is always a force rather than a torque. Thus a combination and arrangement of these actuation forces becomes the primary design consideration. Figure 5.18 [27] shows a typical combination and arrangement of actuations for six-axial stage applications. The upper three in-plane actuation forces are combined to generate in-plane motions, i.e., from left to right, x- and y-axial rectilinear motions, and rotation with respect to z-axis. The lower three vertical actuation forces are combined to generate out-of-plane motions, i.e., from left to right, rotations about x and y axes, and translation along z axis. These actuation forces are combined in symmetric manner to create independent motions of the stage, i.e., three independent axial motions and three independent rotations about each axis. Thus the one-to-one mapping between actuation forces and stage motions can be built. Similar layouts of the actuation forces are presented with details in [26].

5.4.2 Kinematics

The kinematics describes the relationship between the stage motions and actuation input motions. Different from conventional mechanisms kinematics such as kinematics of robotics that the kinematics are governed by geometric relationships caused by the rigid links, the kinematics of electro-magnetic nano-positioning systems are difficult to define because the motions are mainly governed by the stiffness of the compliant guiding mechanisms. In other words we need to consider the relationship between input actuation forces and resultant stage motions rather

than only the relationship between input and output motions. In current research, assumptions of linear deformations of compliant guiding mechanisms, small stage displacements, and constant actuation forces over the range of motion are made. Euler's beam theories and Castigliano's second theorem can be used to derive the stiffness of compliant guiding mechanisms that has regular geometries. For irregular geometries, closed-form solutions may be challenging. Numerical solutions such as finite-element analysis may be used to determine the stiffness. Because of these assumptions, matrices are employed for building the input–output linear kinematic mappings.

As in the six-axis positioning stage layout, here, we employ the stiffness matrix K of the compliant guiding mechanism which relates the actuation force $\mathbf{F}$ on the stage to the stage displacements $\mathbf{x}$, as in (5.6) [8]. The actuation force on the stage is related to the actuation force acting on the paddle through force transformation matrix T, and the actuation force on the paddle is related to the input vector $\mathbf{i}$ (voltage, current, etc.) through actuation matrix, K_a. K_a is derived from the electromagnetic analysis. With this, the actuation force on the stage is given by (5.7) [8].

$$\mathbf{F} = K\mathbf{x} \tag{5.6}$$

$$\mathbf{F} = TK_a\mathbf{i} \tag{5.7}$$

Equating (5.6) and (5.7), we derive the system input–output relationships, as in (5.8) [8]. For the objective stage motions, one can calculate the required input vectors using (5.8) if these matrices are invertible. Because the stage center of mass is on the plane of the horizontal actuations, the horizontal and vertical motions are decoupled.

$$\mathbf{i} = (TK_a)^{-1}K\mathbf{x} \tag{5.8}$$

5.4.3 Dynamics

With the assumption of linear system and lumped stage mass and damping, the dynamics of the system is given by [8]

$$M\ddot{\mathbf{x}} + B\dot{\mathbf{x}} + K\mathbf{x} = TK_a\mathbf{i} \tag{5.9}$$

where M, B, and K are the mass, damping, and stiffness matrices of the system. Coupling between the in-plane and out-of-plane motions generates unwanted erroneous motions and add complexity of control design. It can be decoupled by placing the stage center of mass on the plane of the horizontal actuations. However, as will be presented in later section, in certain applications, the coupling effect cannot be eliminated in this way, and it could only be minimized via control

methods. For most of the nano-positioning systems that are not lumped mass and guided by compliant mechanisms, it is difficult to establish closed-form dynamics equations. However, the dynamics of the system can be identified using simulations and experiments.

5.5   Control

The control of electro-magnetic nano-positioning systems varies with respect to different applications. Thus in this section, we present the control schemes on the typical application of electro-magnetic nano-positioning application, the probe-data storage device, as in Figs. 5.1 and 5.7. In this system [28], a MEMS-based micro-scanner with x/y-directional motions is used to position the storage medium relative to the array of probes so that data is written/read/erased. Each actuator consists of a pair of magnets and a solenoid in the middle. Upon application of a current, one magnet is attracted and the other is repelled by the solenoid, forcing the shuttle to move in the same direction. If the direction of current is altered, the shuttle will be pushed in opposite direction. Before introducing the control schemes, we first present sensors that are used to provide the positional information of the micro-scanner.

5.5.1   Position Sensors

5.5.1.1   Thermal Position Sensors

The working principle of the thermal positional sensors is depicted in Fig. 5.19 [29]. The devices have the form of "U"-shaped cantilever, which consists of two supporting legs and one resistive heater in-between. The devices are made from single-crystal silicon using standard bulk micromachining technology. The resistive heater is made from moderately doped silicon, whereas the legs are made from the highly doped silicon. When applied a voltage on the legs, current flows through the heater resulting in temperature increases of the device. To ensure a uniform temperature increases along the resistive heater, the legs are usually fabricated with equal length.

Figure 5.19c, d illustrates the working principle of the thermal position sensor. To use the device as a position sensor, it should be positioned right above the surface of the object of interest and the surface of the sensor should be parallel to the object surface. Since the larger the overlapped area between the sensor and the underlying object leads to more efficiency in cooling, the temperature of the sensor should be lower than that of the less overlapped case. On the other hand, the resistance of the sensor increases with an increased temperature and decreases with decreased temperature. This variation in resistance can be monitored by looking at the current
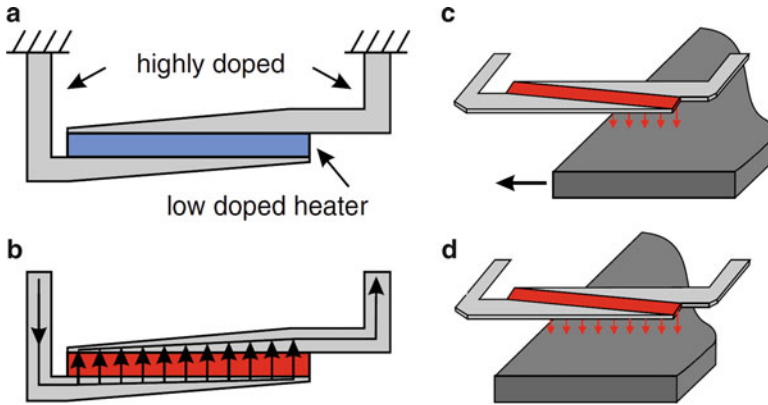
Fig. 5.19 (**a**) Schematic diagram of the thermal position sensor. (**b**) Application of a voltage on the legs results in current flow through the resistive heater. (**c**) The current causes the heat generation of the resistive heater, which is conducted to the underlying surface through the air layer. (**d**) As the underlying surface is moved towards the left, more heat is transferred to the surfaces, which results in temperature decreases of the resistive heater and its electrical resistance accordingly [29]

flowing through the beams. When the sensor is applied by a constant voltage, the change in overlapped area can be thus indirectly detected by measuring the current passing through the sensor. To obtain the position information, the long axis of the resistive heater should be aligned parallel to the direction of motion. Hence, the position can be sensed by monitoring the current flowing through the sensor. Usually for both x and y axial position sensing, two sensors are combined and arranged in orthogonal directions independently. The thermal position sensor of an electro-magnetic nano scanner is shown in Fig. 5.7b.

The single thermal sensor is capable of achieving a satisfactory resolution. However, the sensing results are affected by fluctuation in ambient temperatures and ageing effects owing to dopant diffusion or oxidation. These effects can be minimized by employing a pair of same thermal sensor and make a differential measurement. As shown in Fig. 5.20a, a pair of sensor positioned with an equal overlapped area will give rise to approximately equal cooling of the resistive heaters and therefore equal temperatures and resistances of the devices. As the underlying object displace towards the left, the difference in overlapped areas leads to difference in temperature and resistance of the resistive heater accordingly. In this arrangement, the fluctuation in ambient temperature and ageing effects for both sensors are approximately equal and thus the difference between the resistances will not be affected.

5.5.1.2 Medium-Derived PES

The thermal position sensors provide universal position information with nanometer resolutions. The probe-storage device, on the other hand, provides an alternative
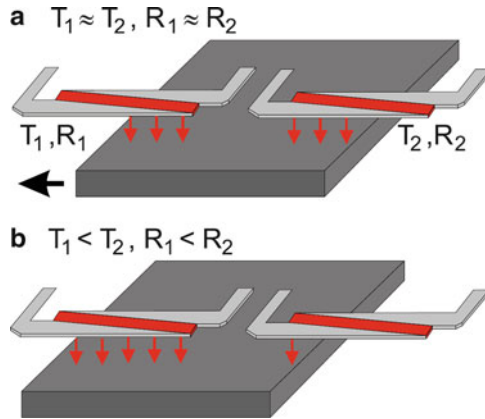
Fig. 5.20 Differential measurement set-up using a pair of matched thermal sensors. (**a**) The test object is positioned between the two thermal sensors leading to equal cooling, and results in approximately equal resistances of the two sensors. (**b**) Because the object is moved towards the left, the cooling of the left sensor increases and the right sensor decreases, and this give rise to a decrease in resistance of the sensor on the left (R_1) and increase of the sensor on the right (R_2) [29]

position sensing technique that is convenient in measuring the deviation of the read/write microcantilever tip from the track center. In addition to data fields, certain storage fields (called servo field) and the corresponding cantilever tips are reserved for generation of position signal, as in Fig. 5.21a. The servo field is shown in Fig. 5.21b, where the circle represents the indentations inscribed prior to the regular operation of the device. The *x*-direction distance of indentations in all bursts is equal to the bit pitch (BP). The cross-track distance between indentations center line of the same burst is equal to the track pitch (TP), whereas the distance between burst centers of A and B (or C and D) is TP/2 [30].

These prewritten indentations provide medium-derived position-error signal (PES), which measures the position deviation in cross-track direction. In regular operations, the track centerline of the data fields is aligned with that of the burst C. Bursts A and B are combined to create the in-phase signal (I-signal), and burst C and D are used to generate quadrature signal (Q-signal). Moreover, the PES is obtained over discrete time step which is needed by the scanner to move a BP in the *x*-direction. Thus the accurately data writing or reading operations along *x*-direction is ensured by medium-derived PES. Compared with the thermal position sensors that are capable of offering absolute position information, the medium-derived PES provides only the relative position deviations in cross-track directions. In other words, the thermal position sensors have a larger range of operation, whereas the medium-derived PES confines to a limited range of sensing. The two sensors provide similar resolutions.
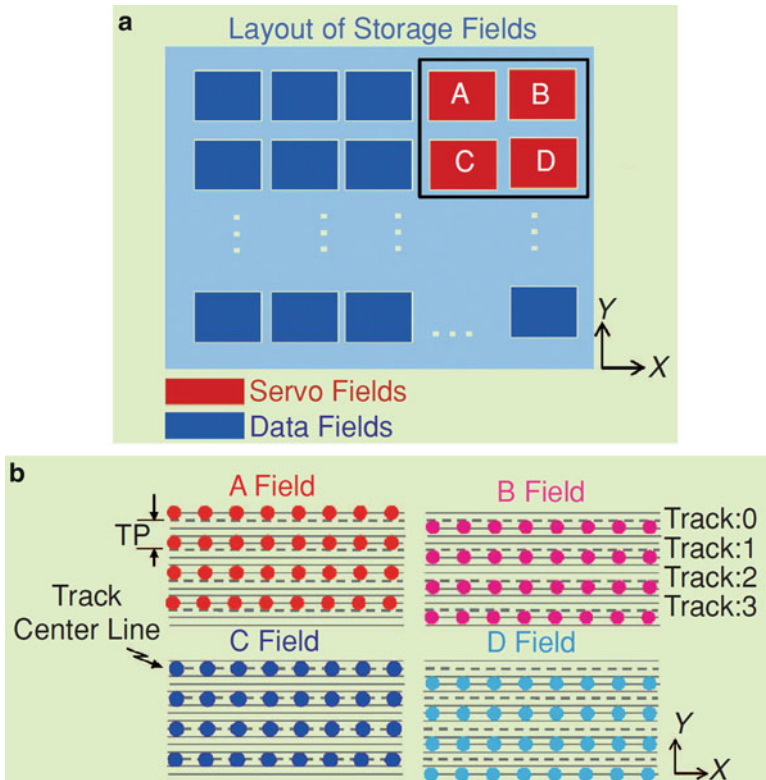
Fig. 5.21 Concept of the medium-derived PES [30]

5.5.1.3 Noise Characteristics

In the absence of external disturbances, positioning accuracy is markedly affected by the noise characteristics of the sensors. For the thermal position sensor, the predominant noise sources are Johnson noise and $1/f$-noise of the silicon resister, whereas the predominant noise sources of the medium-derived PES are medium and channel noise [30]. Moreover, the thermal position sensor suffers from drift and sensitivity variations. The noise spectral characteristics of both the thermal position sensor and medium-derived PES are shown in Fig. 5.22 [30]. As can be seen from Fig. 5.22, there is a significant low-frequency component of the thermal position sensor. This will result in the measurement particularly noisy at low frequencies. In contrast, the medium-derived PES shows good low-frequency fidelity. It should be noted that beyond a certain frequency, performance of the thermal position sensor is better than that of the medium-derived PES.
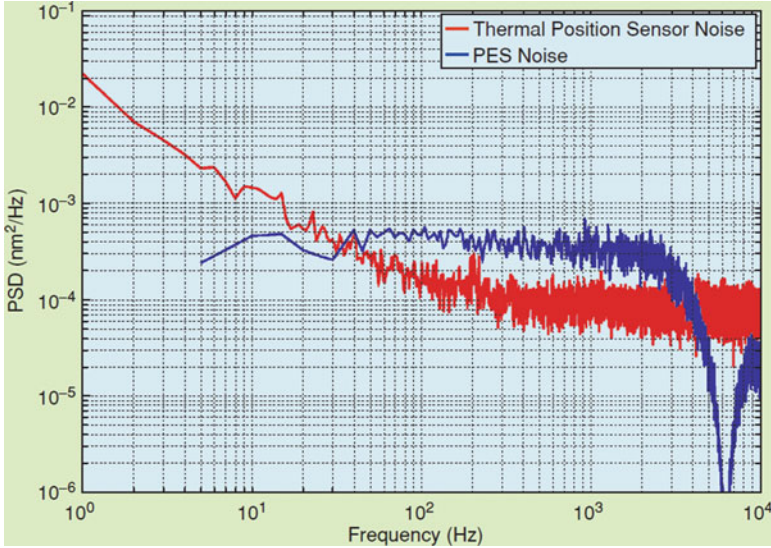
Fig. 5.22 The characteristics of the thermal position sensors and the medium-derived position-error signal (PES) [30]

5.5.2 Control Schemes

The control schemes are based on actual requirements in positioning. As with the PDS devices, the control system has mainly two functions. First, the scan table is to be located to a target track from an arbitrary initial position. This procedure is known as seek-and-settle. Second, from the target position, the medium scanner should be moved with constant velocity along the length of the track along which the writing/reading are operated. The probes should be maintained on the center of the target track while operation. This is achieved by the track-follow procedure.

5.5.2.1 Cross-Coupling

In this planar configuration of the electro-magnetic nano-positioning system, x- and y-directional motion is achieved independently by their respective actuators. However, there are cross-coupling components between the axes in the system owing to the compliant guiding mechanisms. As shown in Fig. 5.23 [31], the cross-coupling is nonlinear and position-dependent. In design of control system, the cross-coupling is usually seen as the disturbance that has to be eliminated by the control.
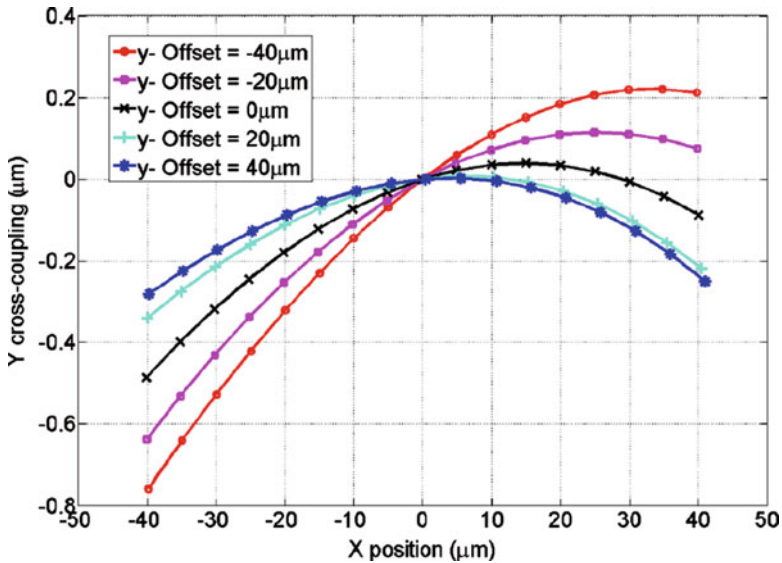
Fig. 5.23 Cross-coupling of *x*- and *y*-axes [31]

5.5.2.2 Seek-and-Settle

The seek-and-settle procedure is essential in data access time, and thus minimizing the duration in this procedure becomes an important control objective. Since medium-derived PES is only capable of providing deviation information in cross-track direction, in this seek-and-settle control procedure the thermal position sensors are thus employed to form a close-loop control scheme. Detailed control architecture can be found in [32].

5.5.2.3 Track-Follow

Different from the seek-and-settle control that the control of *x*- and *y*-directional motions of the scanner is equivalent, the track-follow control exhibits different control requirements in the two axes. As mentioned earlier, the *x*-direction scan should be kept at constant velocity to avoid timing jitter in the readback signal. Fortunately, low-frequency of positioning error is tolerable thanks to the timing-recovery circuits. This makes using the thermal position sensor acceptable despite its unreliability in measurement of errors at low frequencies. For *y*-direction control, the main objective is to maintain the probes to be at the track centerline while scanning in *x*-direction. In achieving this, both the low and high frequencies have to be minimized. The thermal position sensors, therefore, cannot be fully trusted because of the low-frequency noise, drift, and sensitivity variations. However, it is advantageous to use the thermal position sensor due to its virtues of large range and

great precision at high frequencies. To avoid the low-frequency noise induced by using the thermal position sensors, the medium-derived PES can be utilized instead.

The two-sensor-based control strategy [32], also known as the frequency-separated control [15, 30], is usually employed for the track-follow procedure. This control scheme is to achieve best error measurement by using thermal position sensor in high frequencies and the medium-derived PES in low frequencies. Moreover, the medium-derived PES can be exploited to estimate drift and make correction of using thermal position sensor at low frequencies.

5.6 Fabrication

Fabrication of macro-scale electro-magnetic nano-positioners is accomplished based on traditional approaches, and in this section we only focus the fabrication of meso- and micro-scale positioning systems. The fabrication of these positioning systems can be divided into two main parts: fabrication of the micro coil and the compliant guiding mechanisms. The compliant guiding mechanisms or flexure-supported platform is usually fabricated using a standard silicon-on-insulator MEMS (SOI-MEMS) micromachining technology. Figure 5.24 [33] shows the fabrication process of a flexure-supported platform.

In fabrication of the flexure-supported platform, the most important consideration is the thickness of the wafer. Since for planar scanning applications, out-of-plane stiffness should be ensured. In this regard, the wafer should be fabricated thicker. However, thicker wafer increases the etching time as a tradeoff. For out-of-plane applications, the structure should be fabricated more but not too flexible to both ensure out-of-plane motion and eliminate the gravity-induced errors.

Fabrication of micro coil is achieved based on two approaches, as in Fig. 5.25 [10]. One approach uses the patterned micro-mold to fabricate Cu coil with high aspect ratio, shown in Fig. 5.25a. There are various mold materials available such as SU-8, polyimide, photoresist, and silicon, etc. Fabrication procedure consists of mainly three steps: mold patterning, electroplating, and removal of mold. However, fabricating a high aspect ratio mold and removing the mold after electroplating are difficult. Another approach is to fill Cu inside Si trench by electroplating and remove the overflowed Cu using CMP (chemical mechanical polishing). The mold of high aspect ratio Cu coil is easily fabricated using ICP-RIE (inductively coupled plasma reactive ion etching) with high resolution, which ensures a lower resistance coil fabrication. In addition, the flat surface thanks to the CMP makes it much easier for other layers to assemble compared with the conventional approach. The procedure can be divided into three steps: seed layer deposition, electroplating inside Si trench, and CMP.

In constructing the whole system, one approach is to assemble the two chips (one with the micro coil and the other one with the flexible-supported platform)
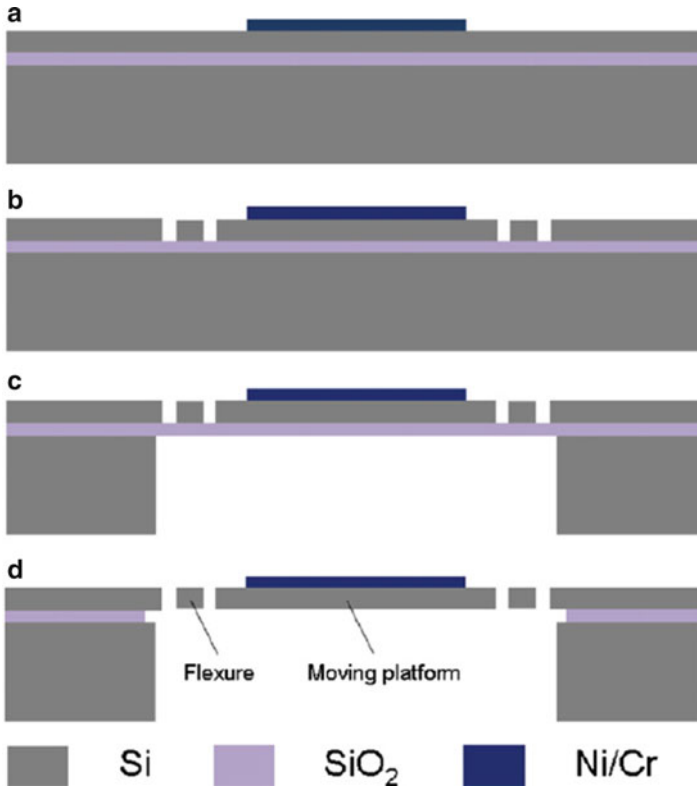
Fig. 5.24 Fabrication process for flexure-supported platform. (**a**) Ni/Cr layer are deposited using liftoff, (**b**) platform shape is etched in the device layer using DRIE, (**c**) handle wafer is etched using DRIE, and (**d**) platform is released by etching the SiO_2 layer in HF and critical point drying [33]

together with the aid of microscope. To ensure high electro-magnetic force, the distance between the coils and magnets should be minimized. Another approach is to integrate the fabrications of micro coils and flexible platform together. The choice of these two approaches depends on different applications.

5.7 Conclusions

Electro-magnetic nano-positioning technology is a relatively young field in nano technologies. This chapter presents a general introduction and guidance on electro-magnetic nano-positioning the aspects covered involve electro-magnetic actuation, guiding mechanisms, system kinematics and dynamics, control, and fabrications. These aspects focus mainly on the most common and general concepts and principles of various electro-magnetic nano-positioning systems. Therefore, potential
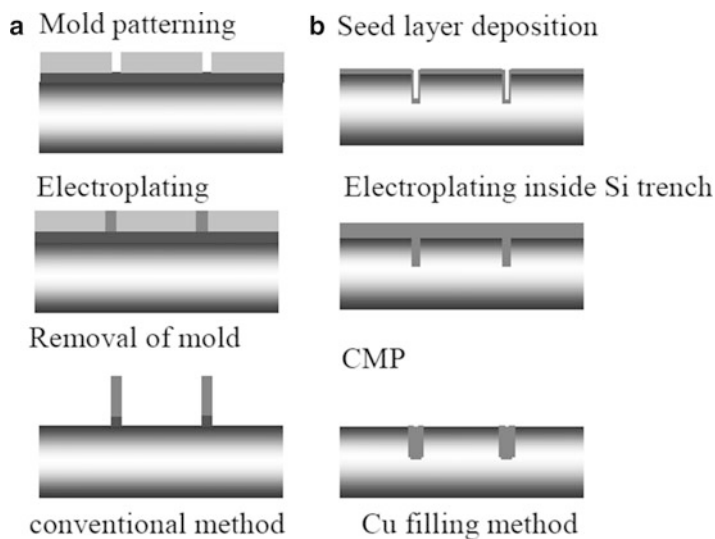
a Mold patterning

b Seed layer deposition

Electroplating

Electroplating inside Si trench

Removal of mold

CMP

conventional method

Cu filling method

Fig. 5.25 Fabrication and process of Cu coil [10]

readers may benefit from it via an overview understanding of the nano-positioning systems. The aim is to provide researchers with guidance on developing high-performance nano-positioning systems for certain applications. In achieving this, a variety of configurations of electro-magnetic nano-positioning systems are reviewed and used as examples to illustrate the related methodologies and technologies. Critical issues for each step in developing the systems are reviewed and summarized. Not limited to current research, this chapter also presents some potential methods such as the pseudo-rigid-body model that may be helpful in the design and analysis of electro-magnetic nano-positioning systems.

References

1. D. Golda, M. Culpepper, Multi-axis electromagnetic moving-coil micro-actuator, in *ASME 2006 International Mechanical Engineering Congress and Exposition*, no. Imece2006-15191 (2006), pp. 57–63
2. G. Haugstad et al., *Scanning Probe Microscopy* (Wiley, 2013)
3. E. Eleftheriou et al., Millipede—a MEMS-based scanning-probe data-storage system. IEEE Trans. Magn. **39**(2), 938–945 (2003)
4. S. Naberhuis, Probe-based recording technology. J. Magn. Magn. Mater. **249**, 447–451 (2002)
5. A. Malshe, K. Virwani, K. Rajurkar, D. Deshpande, Investigation of nanoscale electro machining (nano-EM) in dielectric oil. CIRP Ann. Manuf. Technol. **54**(1), 175–178 (2005)
6. M. Khatib, MEMS-based storage devices: integration in energy-constrained mobile systems. Doctoral Dissertation, University of Twente, 2009
7. M. Khatib, E. Miller, P. Hartel, Workload-based configuration of MEMS-based storage devices for mobile systems, in *Proceedings of the 8th ACM & IEEE Conference on Embedded Software* (October 2008)

8. D. Golda, Design of high-speed, meso-scale nanopositioners driven by electromagnetic actuators. Doctoral Dissertation, MIT, February 2008
9. S. Verma, W. Kim, J. Gu, Six-axis nanopositioning device with precision magnetic levitation technology. IEEE/ASME Trans. Mechatronics **9**(2), 384–391 (2004)
10. J. Choi, H. Park, K. Kim, J. Jeom, Electromagnetic micro x-y stage for probe-based data storage. J. Semicond. Technol. Sci. **1**(1), 84–93 (2001)
11. C. Jaejoon, P. Hong sik, K. Kim, J. Jeon, Electromagnetic micro x-y stage with very thick Cu coil for probe-based mass data storage device. Proc. SPIE **4334**, 363–371 (2001)
12. M. King, B. Zhu, S. Tang, High-precision control of a maglev linear actuator with nanopositioning capability. Mob. Robots **8**(2), 520–531 (2001)
13. W. Kim, H. Maheshwari, High-precision magnetic levitation stage for photolithography, in *Proceedings of the American Control Conference* (2002), pp. 4279–4284
14. W. Kim, D. Trumpert, High-precision planar magnetic levitation. Precis. Eng. 66–77 (1998)
15. A. Pantazi et al., Control of MEMS-based scanning-probe data-storage devices. IEEE Trans. Control Syst. Technol. **15**(5), 824–841 (2007)
16. M. King, B. Zhu, S. Tang, 6-Axis electromagnetically-actuated meso-scale nanopositioner. IEEE Control Syst. Mag. 26–35 (2008)
17. L. Howell, *Compliant Mechanisms* (A Wiley-Interscience Publication, 2001)
18. Q. Xu, Design and development of a flexure-based dual-stage nanopositioning system with minimum interface behavior. IEEE Trans. Autom. Sci. Eng. **9**(3), 554–563 (2012)
19. Y. Yong, S. Moheimani, B. Kenton, K. Leang, Invited review article: high-speed flexure-guided nanopositioning: mechanical design and control issues. Rev. Sci. Instrum. (83) (2012)
20. G. Anderson, A six degree of freedom flexural positioning stage, Masters Thesis, MIT, 1999
21. M. Culpepper, G. Anderson, P. Petri, HEXFLEX: a planar mechanism for six-axis manipulation and alignment. Patent pending, Massachusetts Institute of Technology, Cambridge, 2001
22. M. Lantz et al., A vibration resistant nanopositioner for mobile parallel-probe storage applications. J. Microelectromech. Syst. **16**(1), 130–139 (2007)
23. S. Kota et al., Design of compliant mechanisms: applications to MEMS. Analog Integr. Circ. Sig. Process. **29**, 7–15 (2001)
24. S. Deepak, M. Dinesh, D. Sahu, G. Ananthasuresh, A comparative study of the formulations and benchmark problems for the topology optimization of compliant mechanisms. J. Mech. Robot. **1** (March 2008)
25. M. Bendsoe, O. Sigmund, *Topology Optimization Theory* (Springer, 2013)
26. J. Zhao, K. Zhou, Z. Feng, A theory of degrees of freedom for mechanisms. Mech. Mach. Theory **39**, 621–643 (2004)
27. C. DiBiasio, M. Culpepper, Design and characterization of a 6 degree-of-freedom meso-scale nanopositioner with integrated strain sensing, in *ASPE Proceedings, Design of Precision Machines* (2010)
28. S. Devasia, E. Eleftheriou, S. Moheimani, A survey of control issues in nanopositioning. IEEE Trans. Control Syst. Technol. **15**(5), 802–823 (2007)
29. M. Lantz, G. Binnig, M. Despont, U. Drechsler, *A Micromechanical Thermal Displacement Sensor with Nanometre Resolution*, vol 15 (Institute of Physics Publishing, 2005)
30. A. Sebastian et al., Nanopositioning for probe-based data storage. IEEE Control Syst. Mag. (2008)
31. A. Sebastian et al., Achieving subnanometer precision in a MEMS-based storage device during self-servo write process. IEEE Trans. Nanotechnol. **7**(5), 586–595 (2008)
32. A. Sebastian, A. Pantazi, Nanopositioning with multiple sensors: a case study in data storage. IEEE Trans. Control Syst. Technol. **20**(2), 382–394 (2012)
33. Y. Choi et al., A high-bandwidth electromagnetic MEMS motion stage for scanning applications. J. Micromech. Microeng. **22** (2012)